# Cernox® cryogenic temperature sensor performance after high level neutron irradiation

**S. Scott Courts*** **and Brian R. Courts**

Lake Shore Cryotronics, Inc., Westerville, USA

*Scott.courts@lakeshore.com

**Abstract.** In this research three Cernox® models of cryogenic temperature sensors commercially available from Lake Shore Cryotronics, Inc. were neutron irradiated in a pool reactor. The tested devices consisted of Cernox models CX-1010-SDs, CX-1050-SDs, and CX-1080-SDs. Separate test groups composed of samples of each model were irradiated at room temperature to total fluences of $10^{12}$ n/cm$^2$ to $10^{18}$ n/cm$^2$ in decade steps. Temperature calibrations over each sensor's respective operating temperature range were performed pre- and post-irradiation, with the neutron-induced shifts presented in terms of equivalent temperature shift. Below $10^{14}$ n/cm$^2$, the observed calibration shifts were within the uncertainty of the Cernox® calibrations. At $10^{15}$ n/cm$^2$ and above, the Cernox® temperature sensors continued to operate but with temperature offsets increasing with both increasing fluence and increasing temperature. At the highest fluence of $10^{18}$ n/cm$^2$, the average offsets ranged from +60 mK at 1.4 K to +10 K at 300 K. The results were largely model independent. A fit of the equivalent average temperature offset as a function of total neutron fluence and temperature is presented. This work details the resulting survivability and performance as a function of temperature and total neutron fluence.

## 1. Introduction

For many years high energy physics experiments and applications have been a main driver of cryogenic engineering. Applications including the Future Circular Collider and ITER require high magnetic fields produced by superconducting magnets for particle steering or plasma confinement. These magnets, in turn, require cryogenic cooling systems with temperature monitoring and control to detect and prevent damage due to superconducting magnetic quenches. While it is never the goal to subject the supporting cryogenic infrastructure to radiation, components including temperature sensors are invariably exposed to fringe radiation, which can result in a significant accumulated radiation dose over the lifetime of the project. Gamma radiation and neutron radiation are often used as a predictor of both the survival and accuracy of sensors in the actual radiation environments. Cernox® Resistance Thermometers (CxRTs) are a widely used cryogenic temperature sensor in applications combining high radiation with high magnetic fields. CxRTs are a negative temperature coefficient, cryogenic thermometer commercially developed by Lake Shore Cryotronics, Inc. (LSCI) [1] as a radiation hard cryogenic temperature sensor for use in the Superconducting Super Collider. [2] Limited research has investigated the radiation hardness of CxRTs in neutron radiation environments at relatively low

levels. [3-6] This research examines the neutron radiation-induced calibration offsets of three CxRT models subjected to neutron fluences ranging from $10^{12}$ n/cm$^2$ to $10^{18}$ n/cm$^2$.

## 2. Experimental Design

Three CxRT model types manufactured by LSCI were tested in this research – models CX-1010-SD, CX-1050-SD and CX-1080-SD. All are composed of a conducting ZrN and non-conducting ZrO matrix with the ratio tailored to provide optimized resistance versus temperature response over their targeted temperature range with the model CX-1010 having the lowest resistance and temperature sensitivity and the model CX-1080 having the highest. Detailed information for each model can be found at [3]. Prior to neutron irradiation, a total of 40 devices of each model type were calibrated over the 1.4 K – 325 K temperature range for models CX-1010-SDs and CX-1050-SDs, or over the 20 K to 325 K temperature range for the model CX-1080-SDs. All calibrations were performed in LSCI's Temperature Calibration Facility. During calibration, the resistance of each device was measured and recorded at either 84 temperatures (models CX-1010-SD and CX-1050-SD) or at 52 temperatures (model CX-1080-SD) spanning their respective temperature ranges. A description of the calibration facility and procedures can be found in [7]. The uncertainties of the calibration measurements are listed in Table 1 by model and temperature.

**Table 1.** Uncertainty of LSCI CxRT calibrations as a function of temperature.

| Temperature (K) | Calibration Uncertainty (mK) by model | | |
|---|---|---|---|
| | CX-1010-SD | CX-1050-SD | CX-1080-SD |
| 1.4 | 4 | 4 | N/A |
| 4.2 | 4 | 4 | N/A |
| 10 | 5 | 4 | N/A |
| 20 | 10 | 8 | 8 |
| 30 | 14 | 9 | 9 |
| 50 | 18 | 12 | 11 |
| 100 | 29 | 17 | 14 |
| 200 | 53 | 31 | 24 |
| 300 | 78 | 46 | 36 |

Following their initial calibration, the 40 devices of each model type were divided into eight groups of five devices each for seven different irradiation levels plus an unirradiated control group. All neutron irradiations were performed by The Ohio State University Nuclear Reactor Laboratory (OSU NRL) in their Research Reactor Auxiliary Irradiation Facility (AIF) resulting in a uniform neutron spectrum for all irradiation levels. The differential neutron flux versus neutron energy spectrum for the AIF measured at 450 kW is shown in Figure 1. As stated by OSU NRL personnel, the flux varies linearly with operating power, but the shape of the spectrum does not change (Kevin Herminghuysen, OSU NRL Senior Researcher, personal communications, August 14, 2024.).

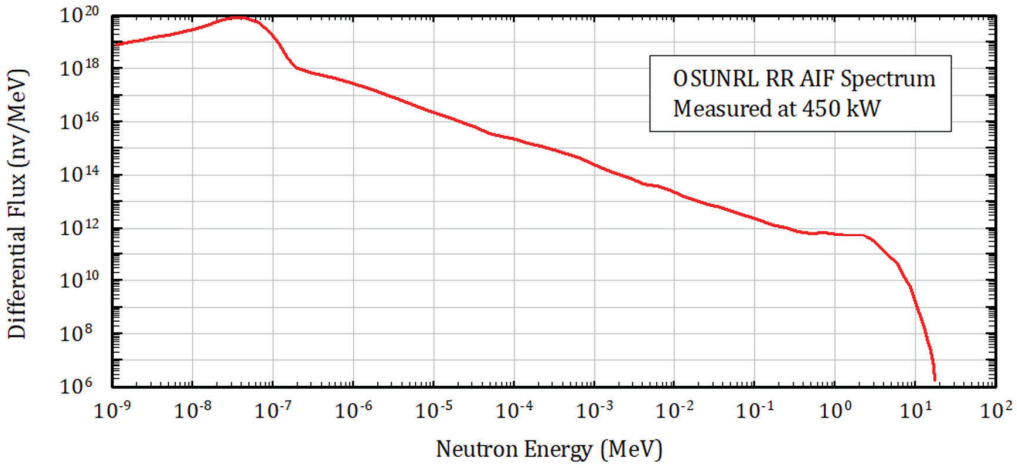


**Figure 1.** Differential Flux versus Neutron Energy for the OS NRL Research Reactor AIF.

The seven neutron irradiation levels chosen for this work were $10^{12}$ n/cm$^2$, $10^{13}$ n/cm$^2$, $10^{14}$ n/cm$^2$, $10^{15}$ n/cm$^2$, $10^{16}$ n/cm$^2$, $10^{17}$ n/cm$^2$ and $10^{18}$ n/cm$^2$. The irradiation levels were limited to $10^{18}$ n/cm$^2$ on the high end due to a combination of (1) CxRT package material activation and required decay time, and (2) maintaining a reasonable irradiation timeframe in the AIF. Devices being irradiated to the same neutron fluence were all placed in a small aluminum canister for the irradiation process. No attempt was made to mount the devices in a particular orientation relative to the reactor core. During the irradiations, the reactor power was varied as necessary to maintain a reasonable irradiation timeframe. The reactor power and irradiation duration for each fluence level are given in Table 2. The estimated dose rate is 686 Gy/hour (Si) when the reactor is operated at 450 kW (Susan White, OSU NRL Senior Researcher, personal communications, April 2, 2025).

**Table 2.** Neutron irradiation parameters for this work.

| Fluence (n/cm$^2$) | Power (kW) | Duration (minutes) |
|---|---|---|
| $10^{12}$ | 0.05 | 13.63 |
| $10^{13}$ | 0.5 | 13.63 |
| $10^{14}$ | 5 | 13.63 |
| $10^{15}$ | 25 | 27.27 |
| $10^{16}$ | 300 | 22.73 |
| $10^{17}$ | 450 | 151.5 |
| $10^{18}$ | 450 | 1515 |

Following neutron irradiation, the devices were recalibrated over the same temperature range as their initial calibrations. The devices irradiated to lower fluences up to $10^{15}$ n/cm$^2$ were recalibrated within a month following irradiation. At higher irradiation fluence levels of $10^{16}$ n/cm$^2$ and above, unanticipated package activation required the devices to be stored at The OSU NRL for periods ranging from a few months to 1.5 years allowing the activated isotopes to decay to exempt activity levels prior to release back to LSCI for recalibration.

## 3. DATA

From an end-user perspective, the important performance parameter for CxRTs is the temperature calibration shift resulting from the neutron radiation. With that in mind, the data were analyzed in terms of equivalent temperature shift of the resistance versus temperature response curve from pre- to post-irradiation calibrations using the equation

$$\Delta T(T) = [\, R_{final}(T) - R_{initial}(T) \,] \,/\, S_T(T) \qquad (1)$$

where $R_{initial}$ and $R_{final}$ are the initial and final resistances at temperature $T$ measured during the pre- and post-irradiation calibrations respectively. This equation is valid when the temperature sensitivity, $S_T$, at the given temperature is relatively constant for both calibrations. In the present work, the change in temperature sensitivity remained below 3% in the worst case, which occurred at room temperature for the $10^{18}$ n/cm$^2$ neutron fluence.

It should be noted that of the 105 total irradiated devices tested, only one failed. The failed device, model CX-1050-SD irradiated to $10^{18}$ n/cm$^2$, read open following irradiation. The device radioactivity level has prevented failure analysis, but that will be completed at a future date.

Figure 2 shows the neutron irradiation-induced calibration offsets for neutron irradiation fluences of $10^{12}$ n/cm$^2$, $10^{13}$ n/cm$^2$, and $10^{14}$ n/cm$^2$. Results for the non-irradiated control group are also included in the plot along with the model CX-1050 calibration uncertainty limits. The behavior across all three CxRT models was nearly identical, and the data shown in Figure 2 are the averages across all three CxRT models for each fluence level. For these lower neutron fluence levels, the combined group offset averages are relatively small and below the calibration uncertainty across the calibration temperature range. Note, however, a trend is developing for the $10^{14}$ n/cm$^2$ devices, which exhibited higher calibration offsets at higher temperature.

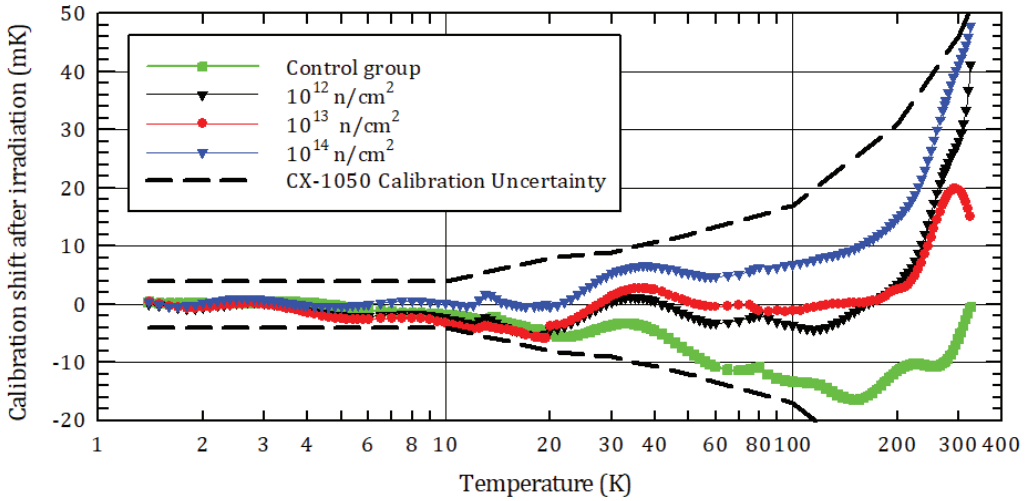


**Figure 2. Combined** Average neutron radiation-induced calibration offsets for three CxRT models with fluence levels of 0 (control group), $10^{12}$ n/cm$^2$, $10^{13}$ n/cm$^2$, and $10^{14}$ n/cm$^2$.

As the neutron fluence was increased to $10^{15}$ n/cm$^2$ and higher, the neutron irradiation calibration temperature shifts all became positive with greater offsets at higher temperatures. Figure 3 shows the offsets for the five CX-1050-SD samples irradiated to $10^{15}$ n/cm$^2$ presented on a log-log scale for better low-temperature resolution. Note the increasing temperature offset with temperature, and, in particular, the near linear temperature offset with temperature response on a log-log scale.

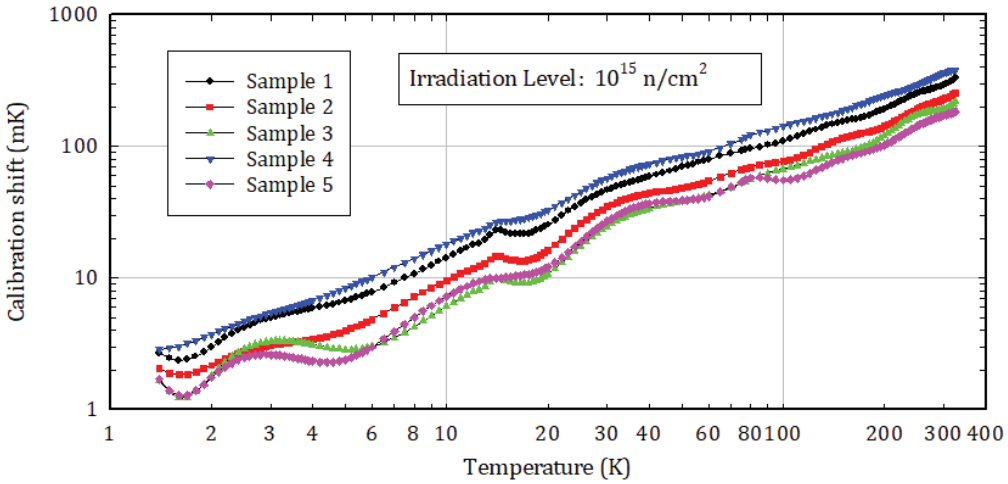


**Figure 3.** Average neutron radiation-induced calibration offsets for the five model CX-1050-SD samples irradiated to a fluence of $10^{15}$ n/cm$^2$.

Figure 4 presents the average offset of each tested CxRT model after irradiation to $10^{15}$ n/cm$^2$. Also plotted are ±1 standard deviation error bars shown for the model CX-1050 average offset, and they encompass the average offsets of both the model CX-1010 and model CX-1080. While not shown in Figure 4, the ±1 standard deviation error bars for all three models overlap, indicating that the neutron irradiation-induced calibration offset is mainly independent of the specific CxRT model.

Figure 5 presents the neutron irradiation-induced calibration offsets for the four highest levels of irradiation. The data are delineated by CxRT model type and fluence, but the pattern observed at the $10^{15}$ n/cm$^2$ extends to the higher irradiation levels. First, the temperature shifts are all in the positive temperature offset direction. Second, the calibration shifts are largely independent of model for a given fluence. For that reason, all devices irradiated to a given fluence were treated as a single group for analysis purposes, and the regression fit for the calibration offset is plotted as a black dashed line for each fluence level in Figure 5. Third, the calibration shifts are nearly linear with temperature on a log-log scale. In fact, the slope of the linear regression fits of the calibration shifts versus temperature for these four highest fluence levels are nearly parallel. Figure 6 shows the intercept, b0, and slope, b1, of each fluence level linear regression fit versus the fluence. It's evident that the slope, b1, of all fits is nearly constant with a value of 0.91±0.04. The intercepts, b0, of the regression fits can be nicely fit as a quadratic dependent only on the fluence level, *F*, as

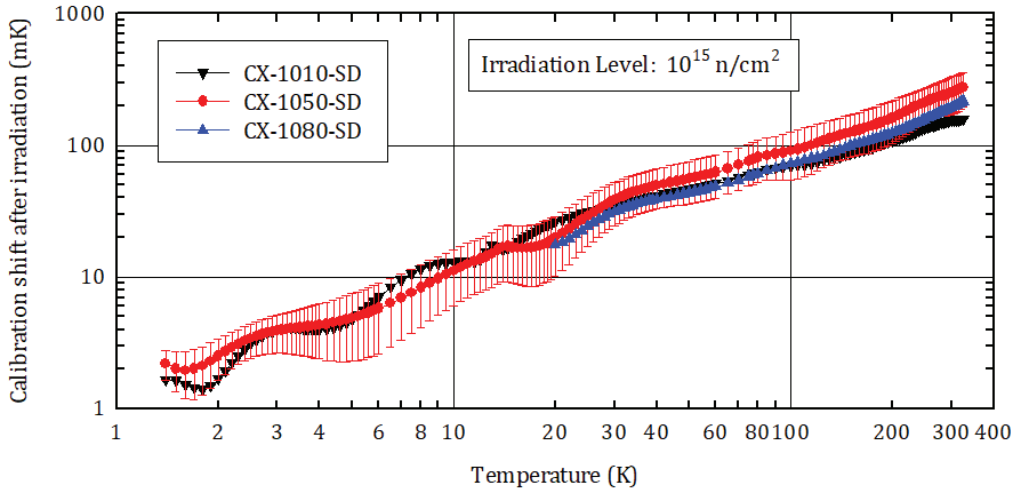


**Figure 4.** Average neutron radiation-induced calibration offsets for each tested CxRT model irradiated to a fluence of $10^{15}$ n/cm$^2$. Included are ±1 standard deviation error bars about the CX-1050-SD average offset.

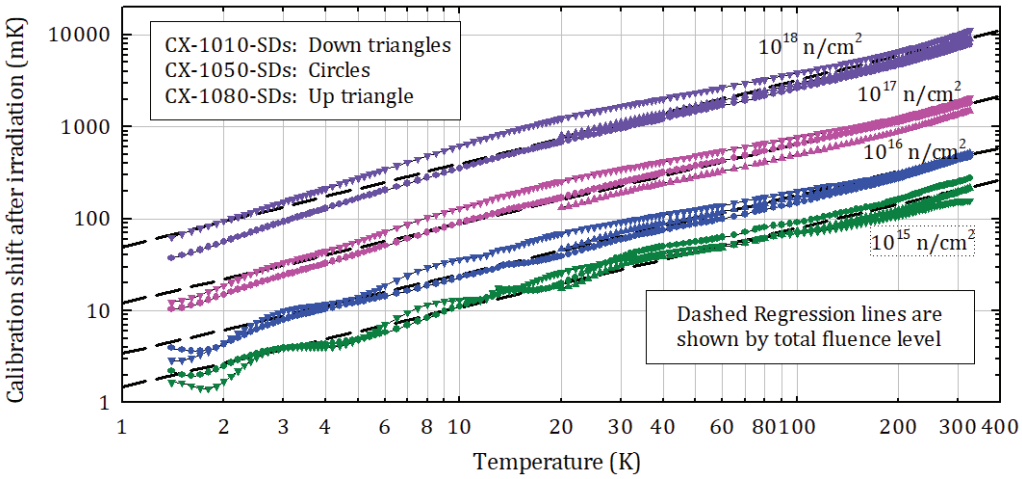


**Figure 5.** Average neutron radiation-induced calibration combined offsets for three CxRT models with fluence levels ranging from $10^{15}$ n/cm$^2$ to $10^{18}$ n/cm$^2$.

$$b_0(F) = (8.7904) + (-1.4589) \times \mathrm{Log}_{10}(F) + (0.0587) \times [\mathrm{Log}_{10}(F)]^2. \qquad (2)$$

Overall, for the four higher neutron fluences, the radiation-induced calibration shifts, $\Delta T$, can be empirically modelled as

$$\mathrm{Log}_{10}(\Delta T) = (0.91) \times \mathrm{Log}_{10}(T) + b_0(F) \qquad (3)$$

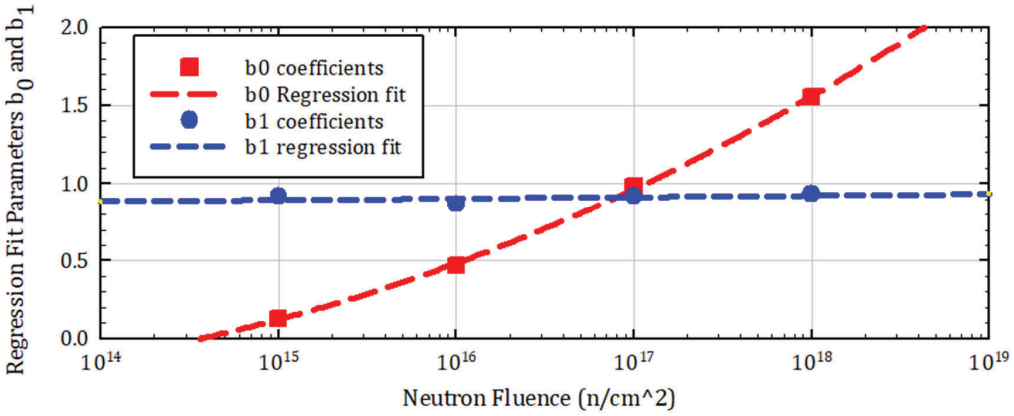


**Figure 6**. Calibration shift linear regression parameters as a function of neutron fluence.

where $T$ is the temperature and $b_0(F)$ is given by Eqn. 2. Eqn. 3 allows prediction of the resulting CxRT calibration shift at a given temperature following neutron irradiation to a specified fluence

Table 3 provides a summary of the average calibration shift and standard deviation at selected temperatures as a function of the neutron fluence for the levels tested in this research.

**Table 3.** CxRT average calibration shift (standard deviation) at selected temperatures for the fluence levels tested in this work.

| | Average Radiation-Induced Calibration Shift (mK) at Neutron Fluence (Standard deviation in mK shown in parentheses) | | | | | |
|---|---|---|---|---|---|---|
| Temp (K) | $10^{13}$ n/cm² | $10^{14}$ n/cm² | $10^{15}$ n/cm² | $10^{16}$ n/cm² | $10^{17}$ n/cm² | $10^{18}$ n/cm² |
| 1.4 | 0.3 (0.6) | 0.4 (0.9) | 1.9 (0.7) | 3.4 (1.6) | 11 (1.8) | 42 (22) |
| 4.2 | -1.8 (1.5) | -0.3 (0.4) | 4.2 (1.6) | 11 (4.7) | 40 (7.5) | 151 (78) |
| 10 | -3.2 (2.6) | 0.1 (1.6) | 12 (4.4) | 29 (14) | 110 (24) | 397 (210) |
| 20 | -3.7 (5.0) | -0.4 (8.7) | 21 (8.2) | 52 (23) | 185 (56) | 780 (329) |
| 30 | 1.3 (7.0) | 5.3 (11) | 35 (11) | 74 (28) | 261 (70) | 1,092 (453) |
| 50 | 0.3 (8.7) | 5.4 (16) | 49 (15) | 106 (38) | 379 (90) | 1,637 (661) |
| 77.35 | -0.7 (12) | 6.1 (20) | 66 (22) | 144 (50) | 524 (112) | 2,324 (920) |
| 100 | -1.2 (10) | 6.8 (23) | 78 (26) | 174 (58) | 634 (126) | 2,857 (1,118) |
| 150 | 0.2 (11) | 9.6 (29) | 104 (34) | 234 (70) | 857 (152) | 3,986 (1,530) |
| 200 | 2.5 (14) | 15 (36) | 131 (44) | 296 (77) | 1,087 (183) | 5,173 (1,959) |
| 250 | 12 (21) | 27 (44) | 168 (52) | 374 (87) | 1,346 (213) | 6,477 (2,431) |
| 300 | 20 (37) | 41 (51) | 200 (63) | 456 (94) | 1,630 (250) | 7,928 (2,958) |

## 4. Discussion

The previous analysis was intended to provide a user with the best information regarding how CxRTs would behave after neutron irradiation. From a physical viewpoint, it's interesting to note that at higher fluence levels, the temperature offsets were all positive. Since CxRTs have a negative temperature coefficient, this implies that the sensor resistance decreased following irradiation. A priori, it would be expected that the physical damage from neutrons interacting with the ZrN/ZrO sensing film would result in higher resistances, which would have resulted in negative

temperature shifts. Damage to the contact metallization would also be expected to result in negative temperature shifts. Since the sensors were randomly oriented during irradiation, it's unlikely that the lower resistance is a result of contact metallization being driven into the sensing film by the neutron flux. Neither is the observed temperature shift likely a result of heating during the irradiation process as reactor personnel estimated the temperature to remain below 323 K during irradiation at even the highest irradiation power/flux to $10^{18}$ n/cm$^2$ fluence. The most reasonable cause of the negative temperature shifts is the neutron interaction with the oxygen in the ZrO component of the sensing film. The ZrO is the nonconducting portion of the sensing film and is incorporated in very small percentage relative to the conducting ZrN component. Even small changes in the ZrO percentage of the sensing film would have a significant impact on the resistance versus temperature response curve.

## 5. Conclusions

This work has examined the CxRT calibration shift resulting from neutron irradiation spanning fluences from $10^{12}$ n/cm$^2$ to $10^{18}$ n/cm$^2$. In all cases, the calibration shifts were largely independent of the CxRT model tested. For fluences at or below $10^{14}$ n/cm$^2$, the calibration shifts were within the CxRT calibration uncertainties, which ranged from ±4 mK at 1.4 K to ±78 mK at 300 K. For fluences ranging from $10^{15}$ n/cm$^2$ to $10^{18}$ n/cm$^2$, the calibration shifts increased with fluence, and for each fluence the calibration shifts increased with temperature. An empirical fit has been provided allowing estimation of the calibration shift for a given temperature and fluence. At the highest fluence of $10^{18}$ n/cm$^2$, the calibration shift was less than 250 mK in the critical temperature range of 4.2 K. Most importantly, 104 of the 105 neutron-irradiated CxRT devices continued to operate post-irradiation. The root cause of the one failure will be investigated when the device has sufficiently decayed for release to LSCI. This work demonstrates the stability and survivability of CxRTs in neutron radiation fluences of up to $10^{18}$ n/cm$^2$.

## Acknowledgments

We would like to acknowledge the support of The Ohio State University Nuclear Reactor Laboratory and the assistance of the reactor staff member Kevin Herminghuysen, Senior Researcher, for the irradiation services provided.

## References

[1] Lake Shore Cryotronics, Inc., 575 McCorkle Blvd., Westerville, OH, 43082, USA, www.lakeshore.com.
[2] Courts S S, Swinehart P R, and Holmes D S 1994, "Radiation Resistant Cryogenic Temperature Sensor for the 4 K to 80 K Range," Dept of Energy final report, contract DE-FG02- 90ER81074.
[3] Courts S S, Holmes D S and Swinehart P R 1992 *Temperature: Its Measurement and Control in Science and Industry* vol 6, part 2, ed J F Schooley (New York, AIP) pp 1237-1242.
[4] Courts S S, and Holmes D S, "Effects of cryogenic irradiation on Temperature Sensors" in: *Adv. Cryo. Eng.* 41B (1996).
[5] Junquera T, Amand . F, Thermeau J P, and Casa-Cubillos J, "Neutron irradiation tests of calibrated cryogenic sensors at low temperatures" in *Adv. Cryo. Eng.* **43A**, (1998).
[6] Amand J F, Casa-Cubillos J, Junquera T, and Thermeau J P, "Neutron irradiation tests in superfluid Helium of LHC Cryogenic Thermometers" in *Proc. of the 17th Intl .Cryo. Eng. Conf.*, **43** (1998).
[7] Courts S S and Courts B R, *AIP Conf, Proc,* **3230**, Issue 1, id.040002. https://doi.org/10.1063/5.0237398